The 8th International Electronic Conference on Medicinal Chemistry (ECMC 2022)

01–30 NOVEMBER 2022 | ONLINE

Interaction of monosubstituted paddlewheel diruthenium compounds with proteins: a structural study

Chaired by **DR. ALFREDO BERZAL-HERRANZ**;
Co-Chaired by **PROF. DR. MARIA EMÍLIA SOUSA**

pharmaceuticals MDPI

Aarón Terán [1], Giarita Ferraro [2], Ana E. Sánchez-Peláez [1], Santiago Herrero [1], Antonello Merlino [2,*]

[1] Department of Inorganic Chemistry, Chemistry Faculty, Complutense University, Madrid, Spain
[2] Department of Chemical Sciences, University of Naples Federico II, Naples, Italy.

UNIVERSIDAD COMPLUTENSE MADRID

UNIVERSITÀ DEGLI STUDI DI NAPOLI FEDERICO II

* antonello.merlino@unina.it

Interaction of monosubstituted paddlewheel diruthenium compounds with proteins: a structural study

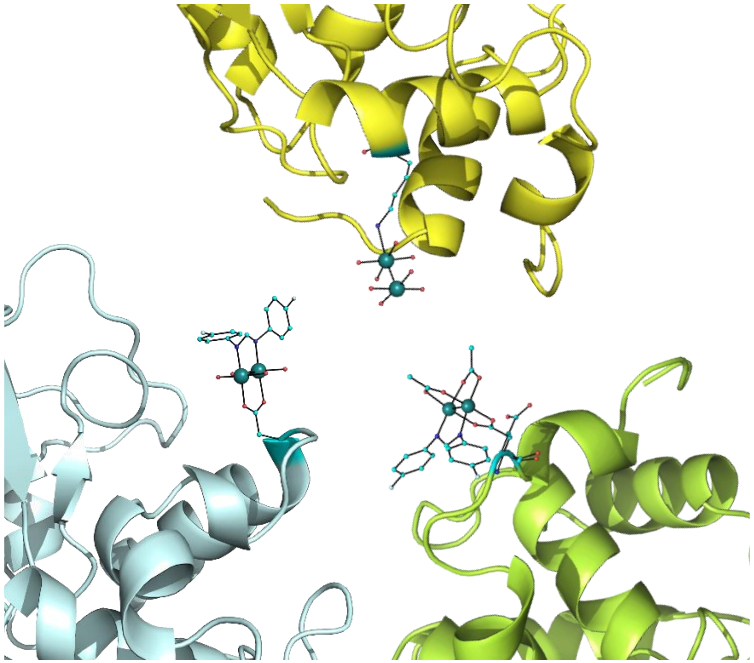

ECMC 2022
The 8th International Electronic Conference on Medicinal Chemistry
01–30 NOVEMBER 2022 | ONLINE

Abstract:
Paddlewheel diruthenium complexes have interesting pharmaceutical properties. The diruthenium tetracetate complex ($[Ru_2Cl(O_2CCH_3)_4]$), the prototype of the diruthenium compound family, has been used to prepare promising anticancer agents (i.e., against glioma tumor models and glioblastoma). The interaction of $[Ru_2Cl(O_2CCH_3)_4]$ with proteins has been already investigated: diruthenium moieties bind Asp side chains upon releasing of one acetate ligand; a second acetate is replaced by two water molecules in each diruthenium center. Recently, it has been suggested that the use of bulky equatorial substituents may constitute an approach to increase the selectivity of diruthenium complexes toward anticancer targets. To study the effect of equatorial ligand replacement on the reactivity of diruthenium compounds with proteins, we solved high-resolution X-ray structures of adducts formed upon reaction of the model protein lysozyme with the monosubstituted complex $[Ru_2Cl(L\text{-}L)(O_2CCH_3)_3]$ (L-L = *N,N′*-bis(4-fluorophenyl)formamidinate). Results indicate that these complexes bind the protein via coordination of the Ru-Ru core to the side chain of Asp residues at the equatorial coordination site, losing only one acetate ligand. Protein binding occurs *cis* or *trans* to the L-L ligands that remain attached to the dimetallic center. The side chain of a Lys and even main chain carbonyl groups can coordinate diruthenium core at the axial site. These data help to understand the reactivity of paddlewheel diruthenium complexes with proteins, providing useful information for the design of new diruthenium compounds with improved pharmacological properties.

Keywords: artificial metalloproteins; paddlewheel diruthenium complexes; protein-metal adducts; ruthenium compounds.

Introduction

Introduction

1957 — 2022

1st compound with a single **M-M** bond

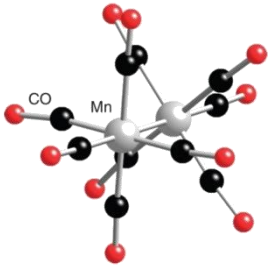

$[Mn_2(CO)_{10}]$

Introduction

1st compound with a multiple **M-M bond**

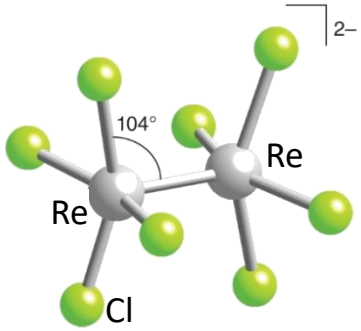

$[Re_2Cl_8]^{2-}$

1957 — 1964 — 2022

1st compound with a single **M-M** bond

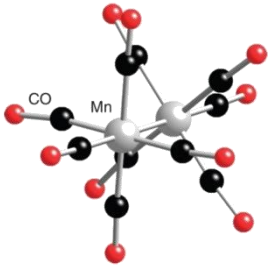

$[Mn_2(CO)_{10}]$

Introduction

1st compound with a multiple **M-M bond**

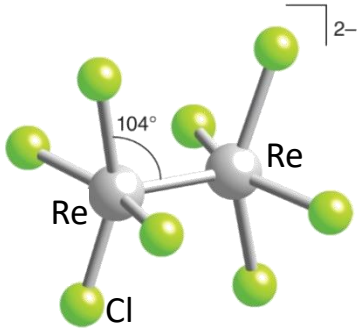

$[Re_2Cl_8]^{2-}$

Molecular compounds with M-M bond

1957 1964 2022

1st compound with a single **M-M** bond

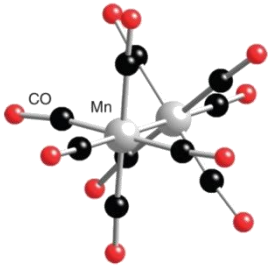

$[Mn_2(CO)_{10}]$

Introduction

1st compound with a multiple **M-M bond**

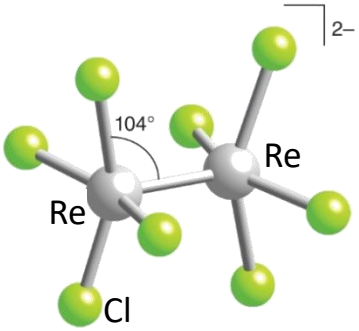

$[Re_2Cl_8]^{2-}$

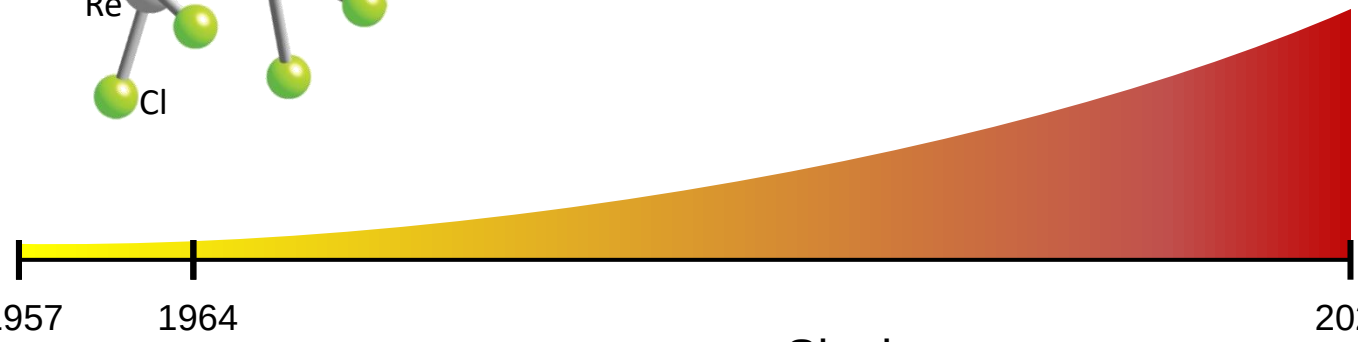

1st compound with a single **M-M** bond

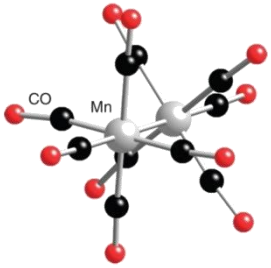

$[Mn_2(CO)_{10}]$

Single or multiple

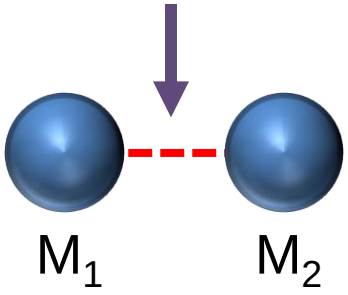

$M_1 = M_2$
$M_1 \neq M_2$

- Transition metals

Introduction

1st compound with a multiple **M-M bond**

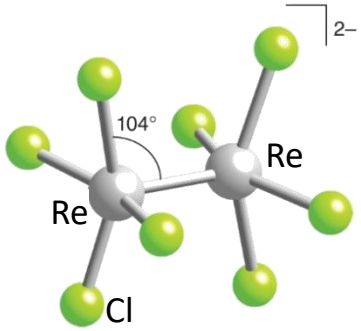

$[Re_2Cl_8]^{2-}$

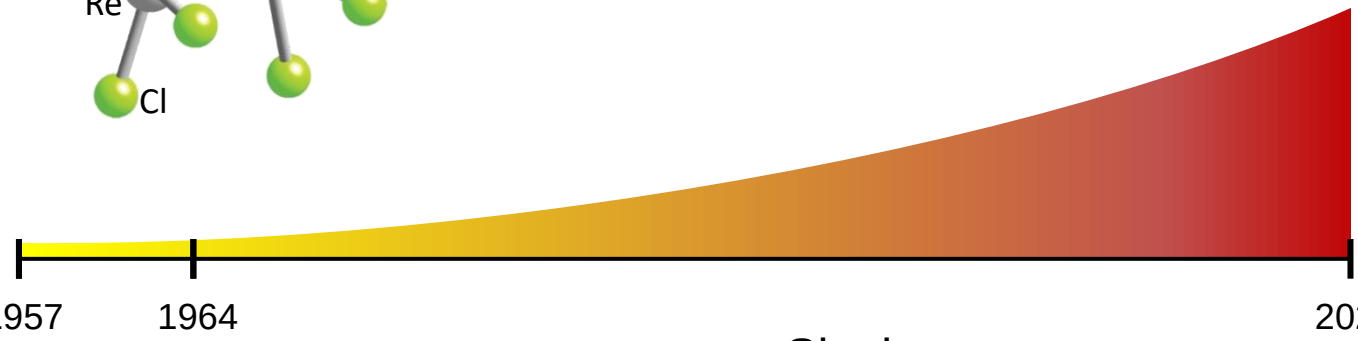

1st compound with a single **M-M** bond

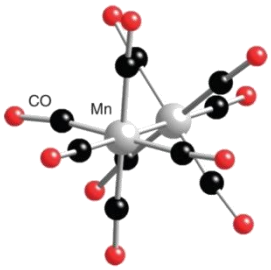

$[Mn_2(CO)_{10}]$

Single or multiple

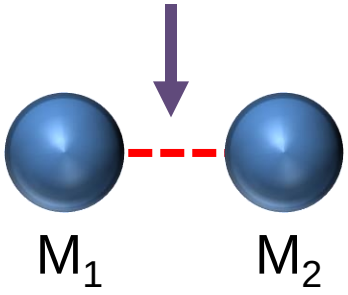

$M_1 = M_2$
$M_1 \neq M_2$

- Transition metals
- *s*-,*p*-,*f*-block elements

Introduction

1st compound with a multiple **M-M bond**

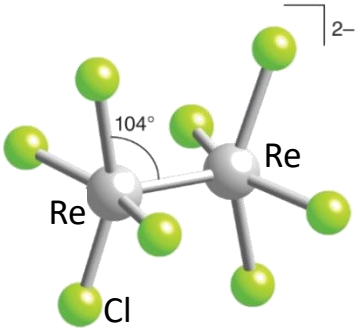

$[Re_2Cl_8]^{2-}$

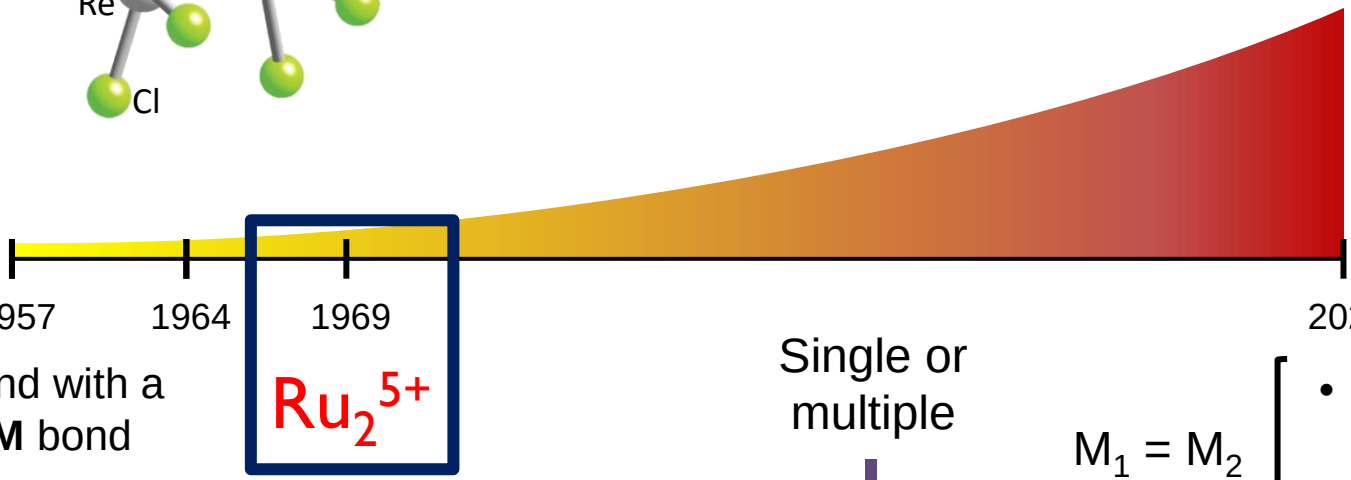

1st compound with a single **M-M** bond

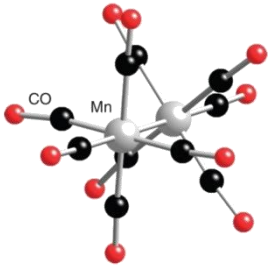

$[Mn_2(CO)_{10}]$

Single or multiple

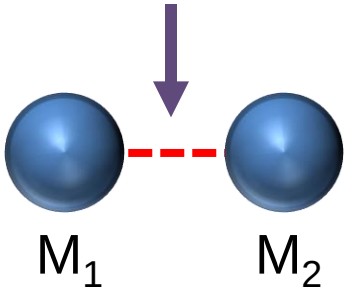

$M_1 = M_2$
$M_1 \neq M_2$

- Transition metals
- *s*-,*p*-,*f*-block elements

Introduction

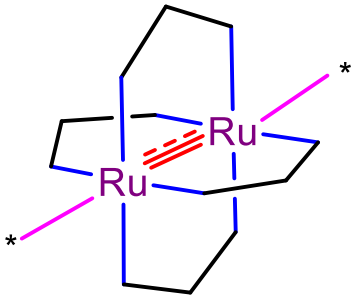

Paddlewheel structure

Equatorial positions

Axial positions

Introduction

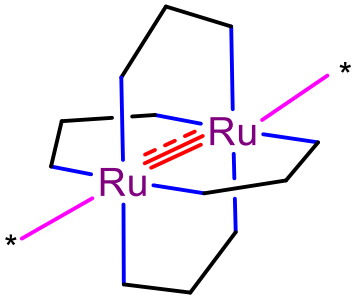

Paddlewheel structure

Equatorial positions

Axial positions

Common ligands

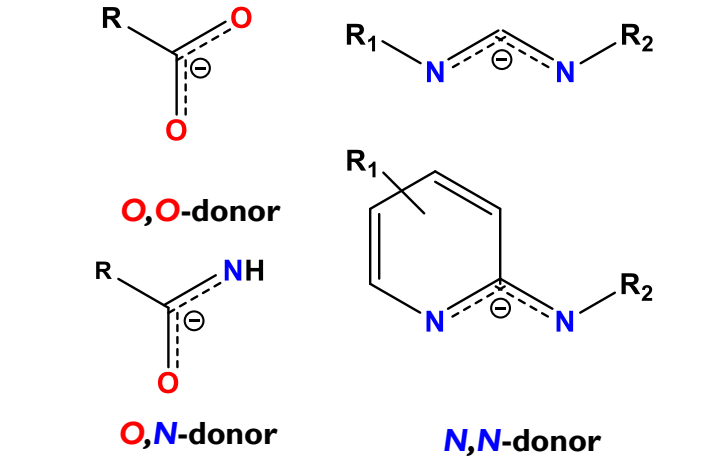

O,*O*-donor

O,*N*-donor

N,*N*-donor

Introduction

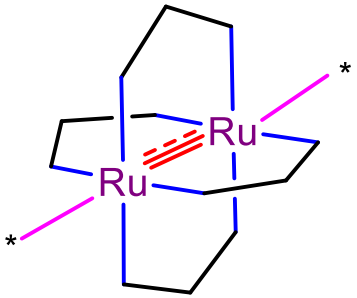

Paddlewheel structure

Equatorial positions

Axial positions

Common ligands

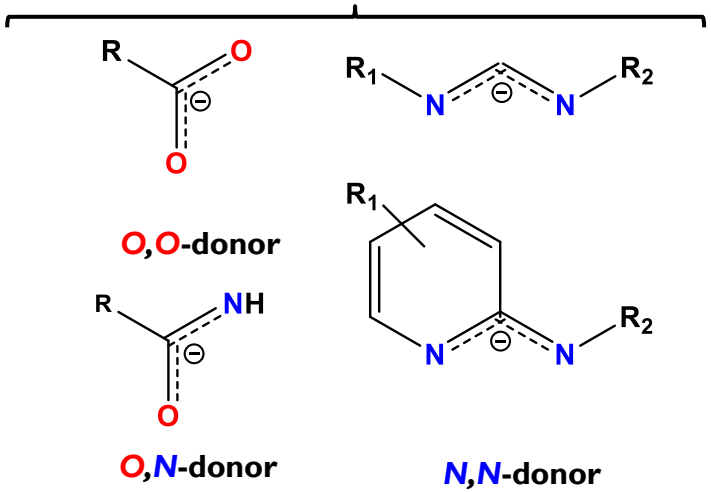

Molecular orbital diagram

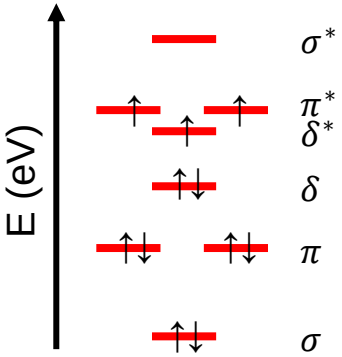

$Ru(II)\text{-}Ru(III) \rightarrow Ru_2^{5+}$

Introduction

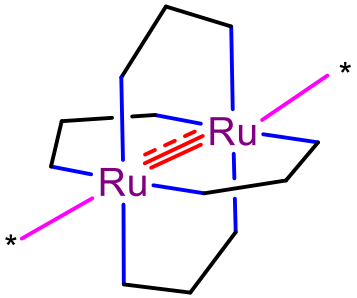

Paddlewheel structure

Equatorial positions

Axial positions

Common ligands

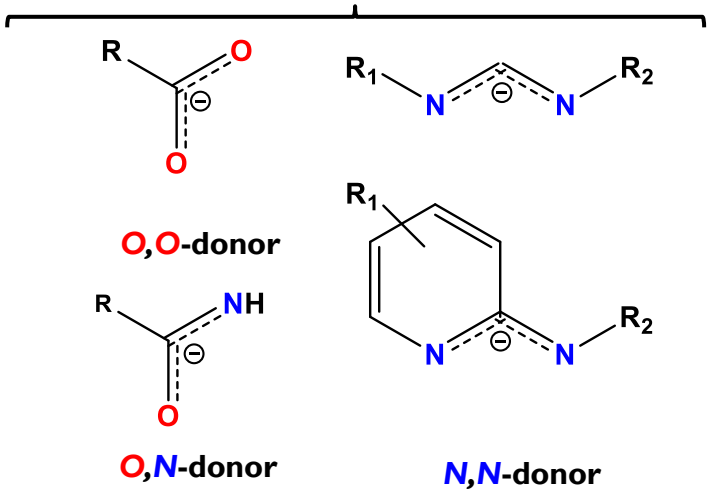

Molecular orbital diagram

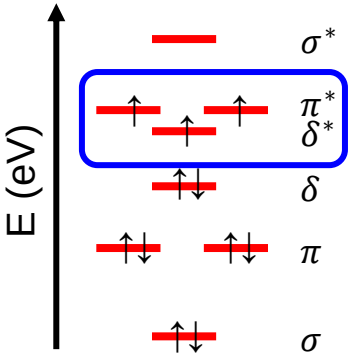

Paramagnetic species

$Ru(II)\text{-}Ru(III) \rightarrow Ru_2^{5+}$

Introduction

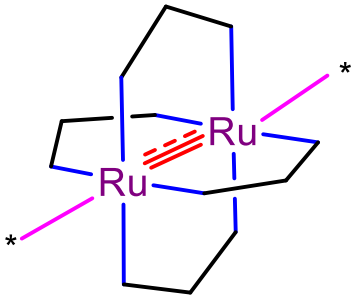

Paddlewheel structure

Equatorial positions

Axial positions

Common ligands

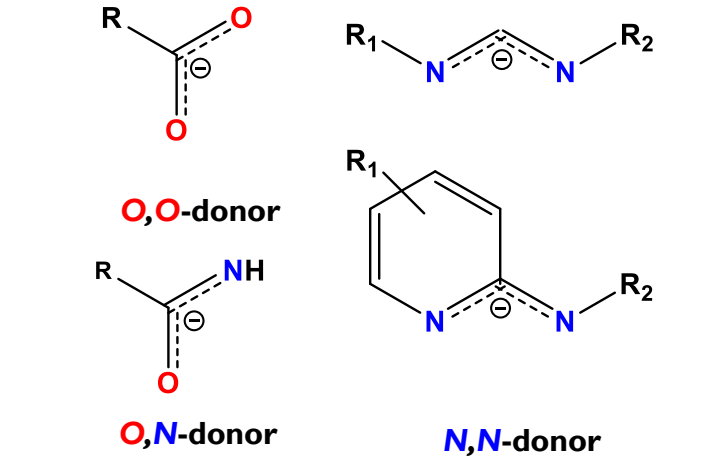

Molecular orbital diagram

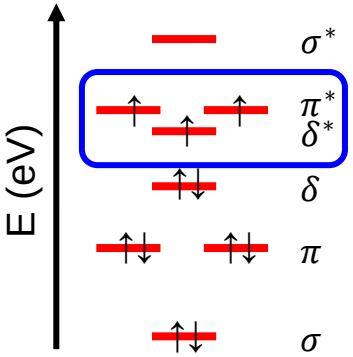

Paramagnetic species

O.E. M-M = 2.5

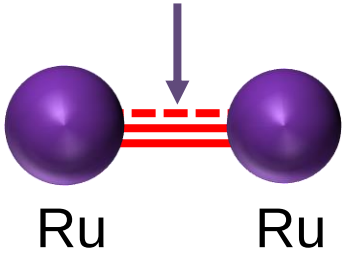

Ru(II)-Ru(III) → Ru_2^{5+}

Introduction

Common starting material

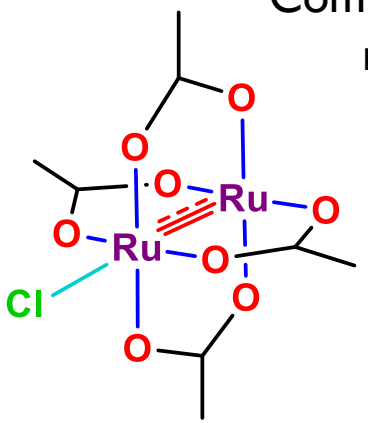

$[Ru_2Cl(O_2CCH_3)_4]$

Introduction

Common starting material

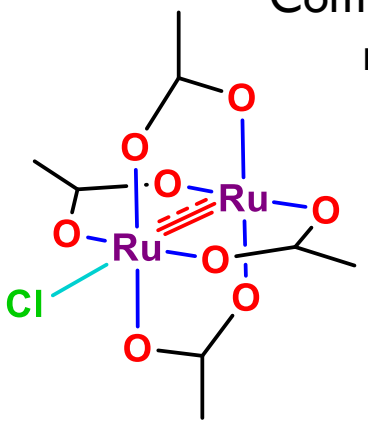

$[Ru_2Cl(O_2CCH_3)_4]$

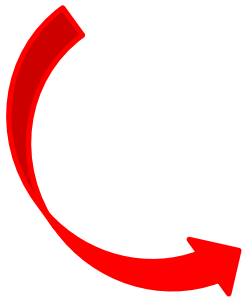

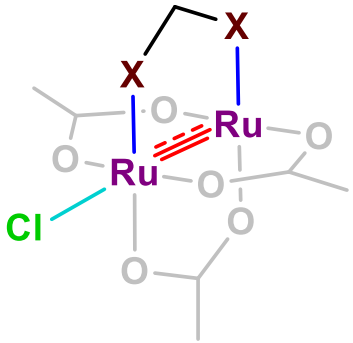

Mono-

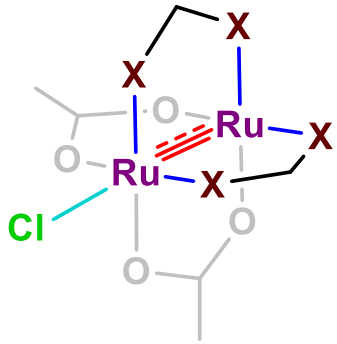

Di-

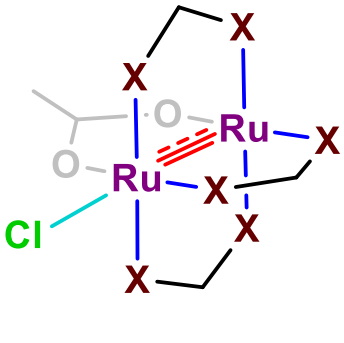

Tri-

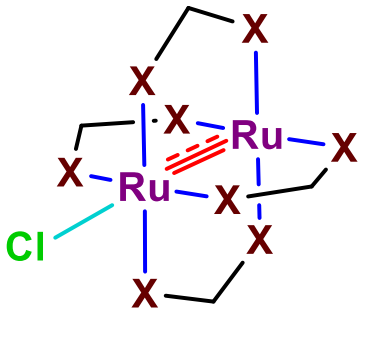

Tetra-

Introduction

Common starting material

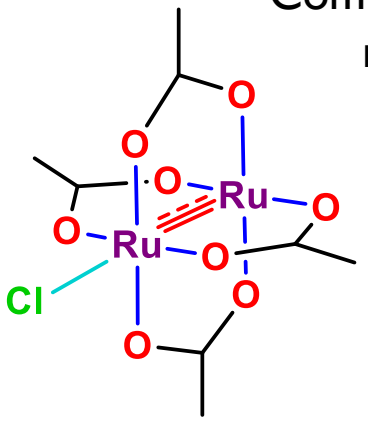

$[Ru_2Cl(O_2CCH_3)_4]$

Biochemistry

Medicinal chemistry

Catalysis

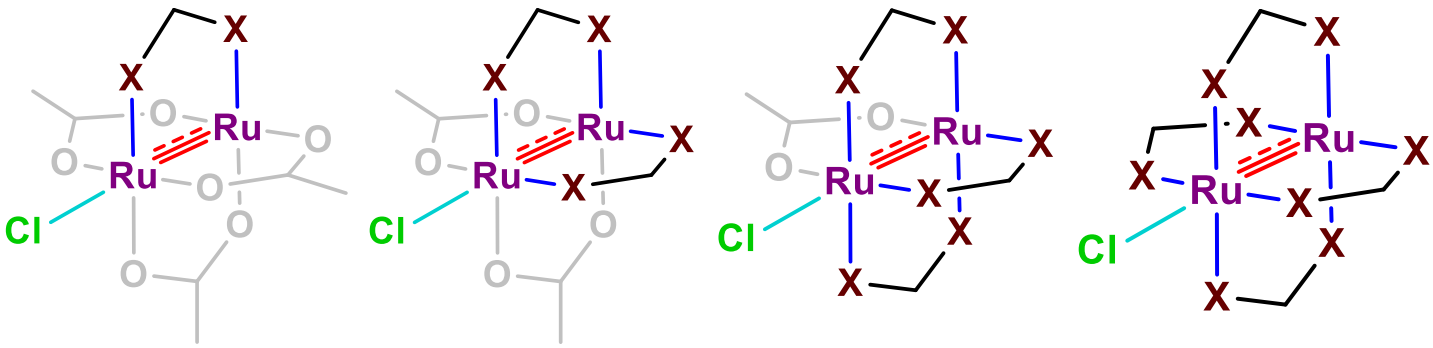

Mono- *Di-* *Tri-* *Tetra-*

Introduction

Common starting material

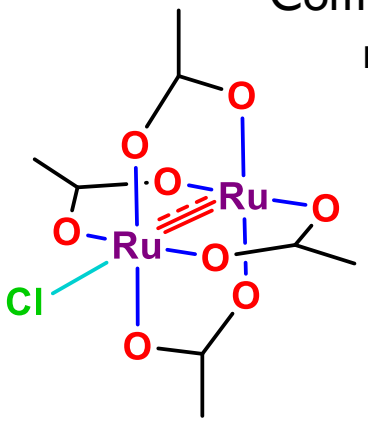

$[Ru_2Cl(O_2CCH_3)_4]$

Biochemistry

Medicinal chemistry

Catalysis

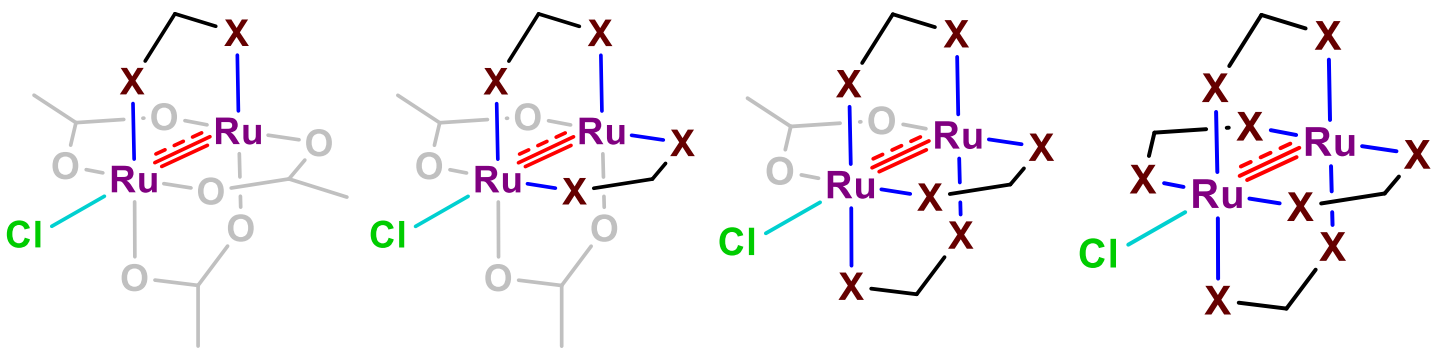

Mono- *Di-* *Tri-* *Tetra-*

Introduction

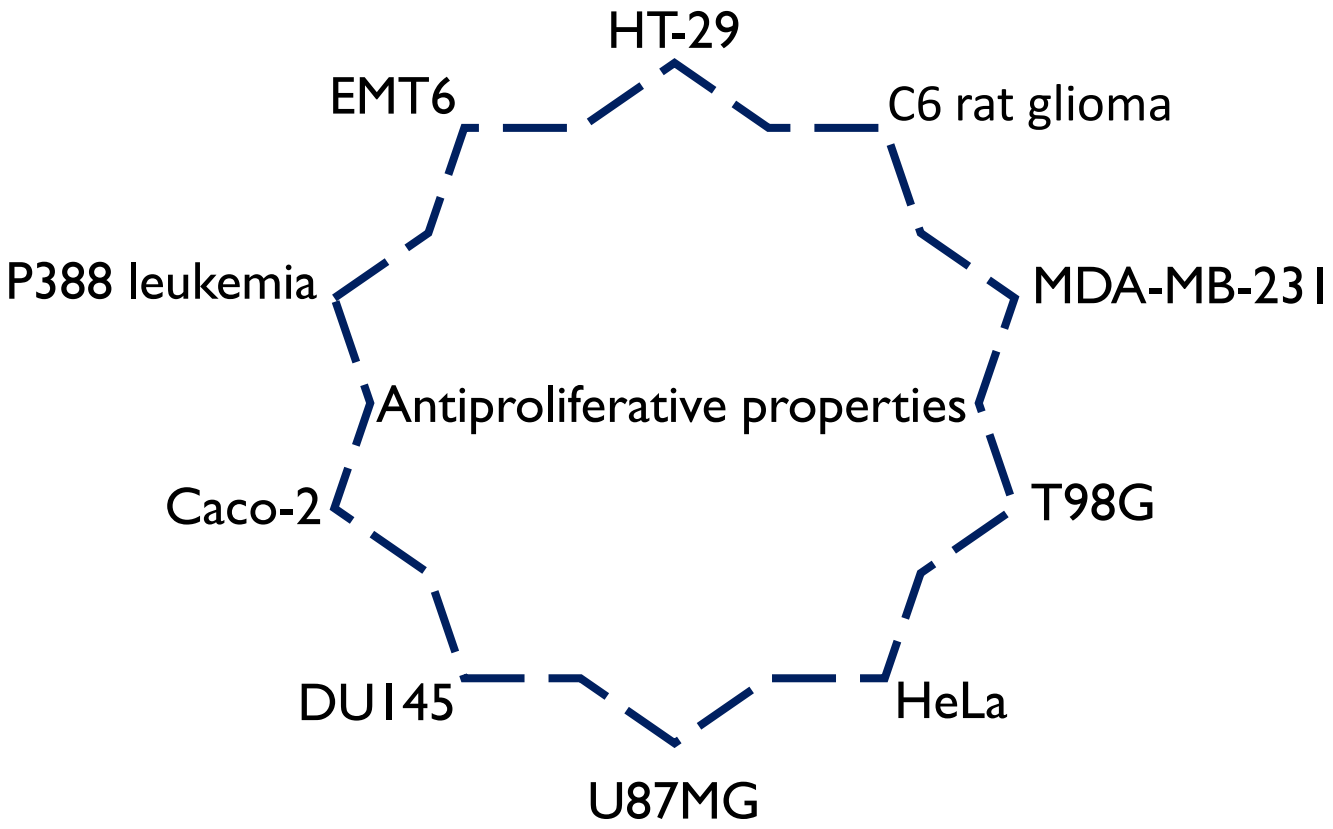

Introduction

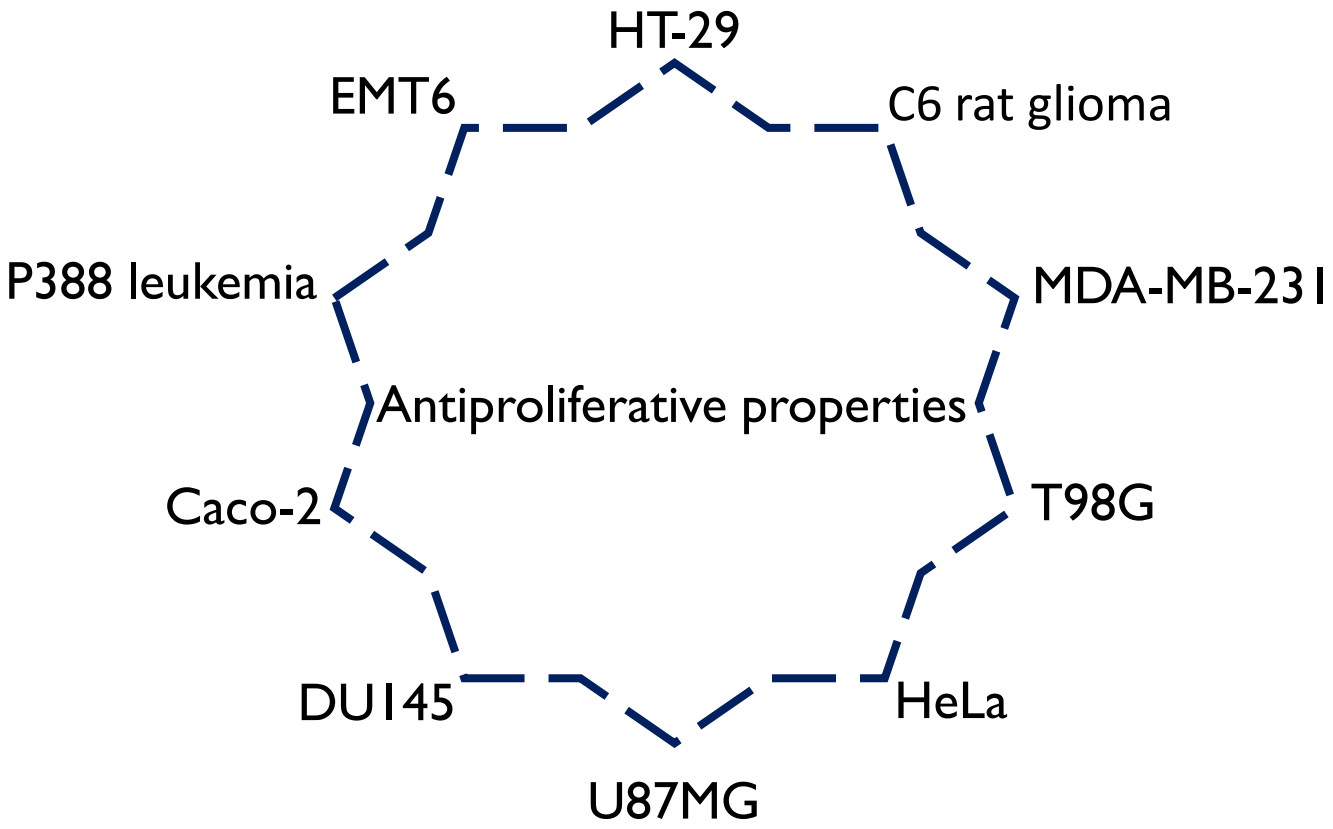

Major problem

↓

Poor water solubility

Introduction

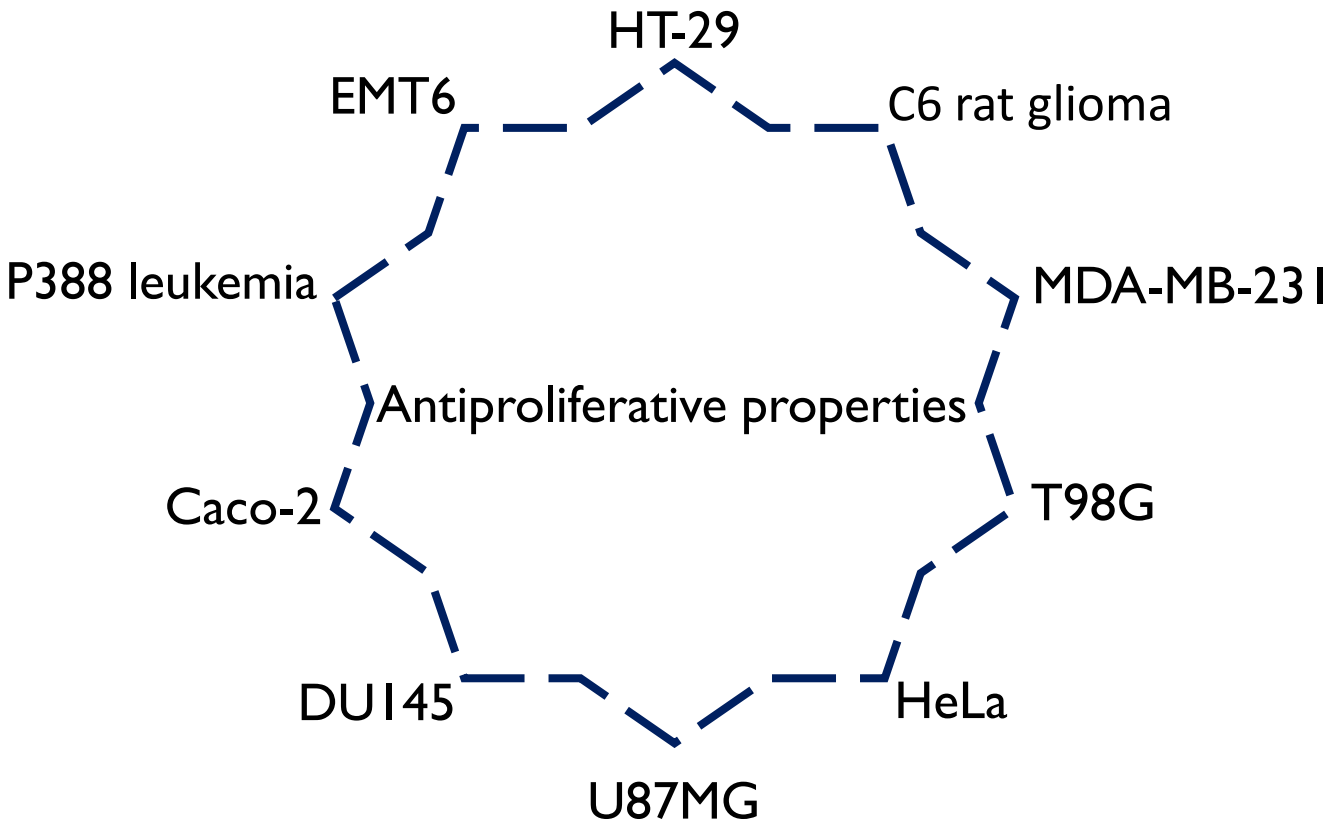

Major problem

↓

Poor water solubility

Solution

↓

Encapsulation techniques

Introduction

Structure – Activity relationship

Angewandte Communications

Metal–Protein Interactions

DOI: 10.1002/anie.201403337

Unusual Structural Features in the Lysozyme Derivative of the Tetrakis(acetato)chloridodiruthenium(II,III) Complex**

Luigi Messori, Tiziano Marzo, Rute Nazaré Fernandes Sanches, Hanif-Ur-Rehman, Denise de Oliveira Silva,* and Antonello Merlino**

Journal of Coordination Chemistry, 2015
Vol. 68, Nos. 17–18, 3209–3228, http://dx.doi.org/10.1080/00958972.2015.1074684

Spectroscopic studies on interactions of the tetrakis(acetato) chloridodiruthenium(II,III) complex and the Ru_2(II,III)-NSAID-derived metallodrugs of ibuprofen and ketoprofen with human serum albumin

RODRIGO LUIS SILVA RIBEIRO SANTOS[1,2], RUTE NAZARÉ FERNANDES SANCHES[2] and DENISE DE OLIVEIRA SILVA*

Dalton Transactions

Dalton Trans., 2021, **50**, 9643–9647 | **9643**

Two mixed valence diruthenium(II,III) isomeric complexes show different anticancer properties†

Elisabetta Barresi, ‡[a,c] Iogann Tolbatov, ‡[b] Tiziano Marzo, *[a,c] Elisa Zappelli,[a] Alessandro Marrone,[d] Nazzareno Re,*[d] Alessandro Pratesi,[e] Claudia Martini,[a,c] Sabrina Taliani,*[a,c] Federico Da Settimo[a,c] and Diego La Mendola[a]

Proposal

Design and synthesis of novel Ru_2 compounds

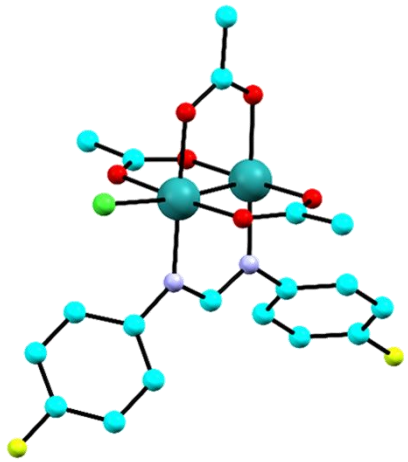

$[Ru_2Cl(L\text{-}L)(O_2CCH_3)_3]$

L-L = *N,N'*-bis(4-fluorophenyl)formamidinate

Stable and soluble in water

Proposal

Design and synthesis of novel Ru_2 compounds

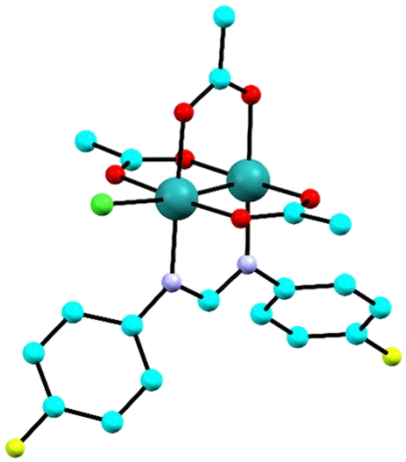

$[Ru_2Cl(L\text{-}L)(O_2CCH_3)_3]$

L-L = *N,N'*-bis(4-fluorophenyl)formamidinate

Stable and soluble in water

Reactivity studies of $[Ru_2Cl(L\text{-}L)(O_2CCH_3)_3]$ with HEWL

High-resolution X-ray crystallography

Results and discussion

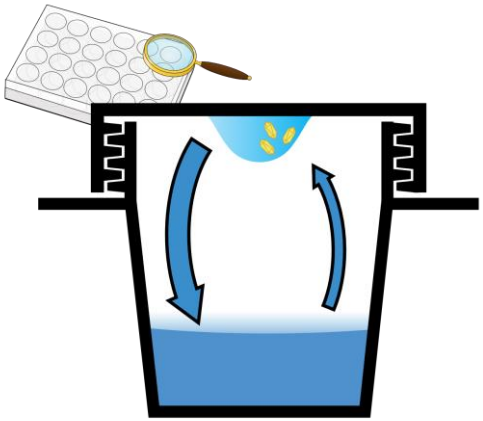

Hanging drop vapor diffusion

Structure A	Structure B	Structure C
2 M HCOONa 0.1 M HEPES buffer (pH 7.5)	20 % Ethylene glycol CH_3COONa buffer (pH 4) $NaNO_3$ 0.6 M	0.8 M Succinic acid (pH 7)

Results and discussion

Soaking

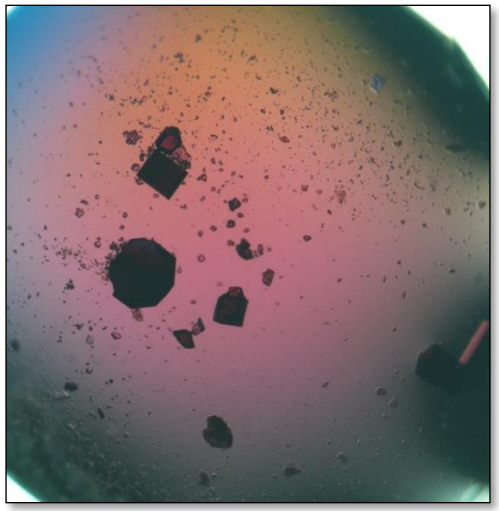

Structure A	Structure B	Structure C
2 M HCOONa 0.1 M HEPES buffer (pH 7.5)	20 % Ethylene glycol CH_3COONa buffer (pH 4) $NaNO_3$ 0.6 M	0.8 M Succinic acid (pH 7)

Results and discussion

Structure A

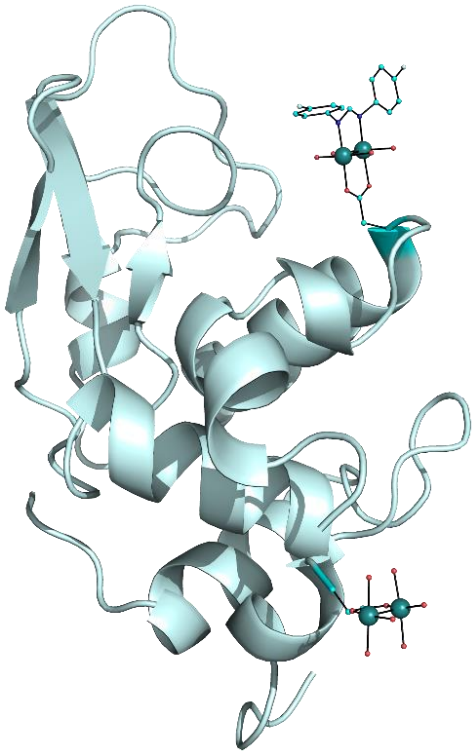

Resolution	R-factor (R-free)	Condition
1.81 Å	0.223 (0.283)	2 M HCOONa, 0.1 M HEPES buffer (pH 7.5)

Results and discussion

Structure A

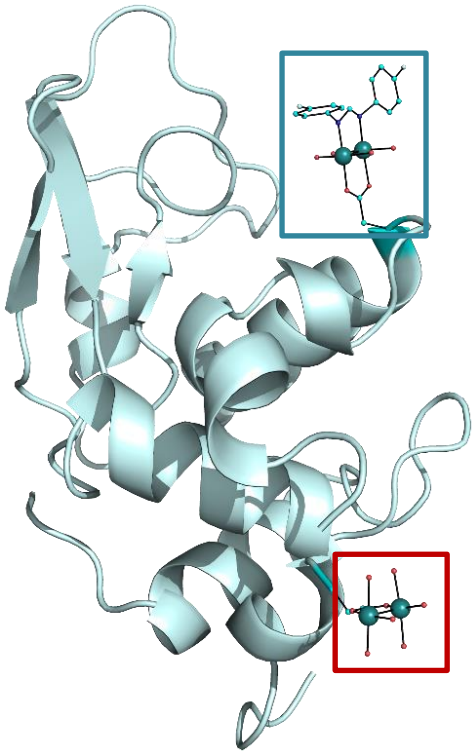

Resolution	R-factor (R-free)	Condition
1.81 Å	0.223 (0.283)	2 M HCOONa, 0.1 M HEPES buffer (pH 7.5)

Results and discussion

Structure A

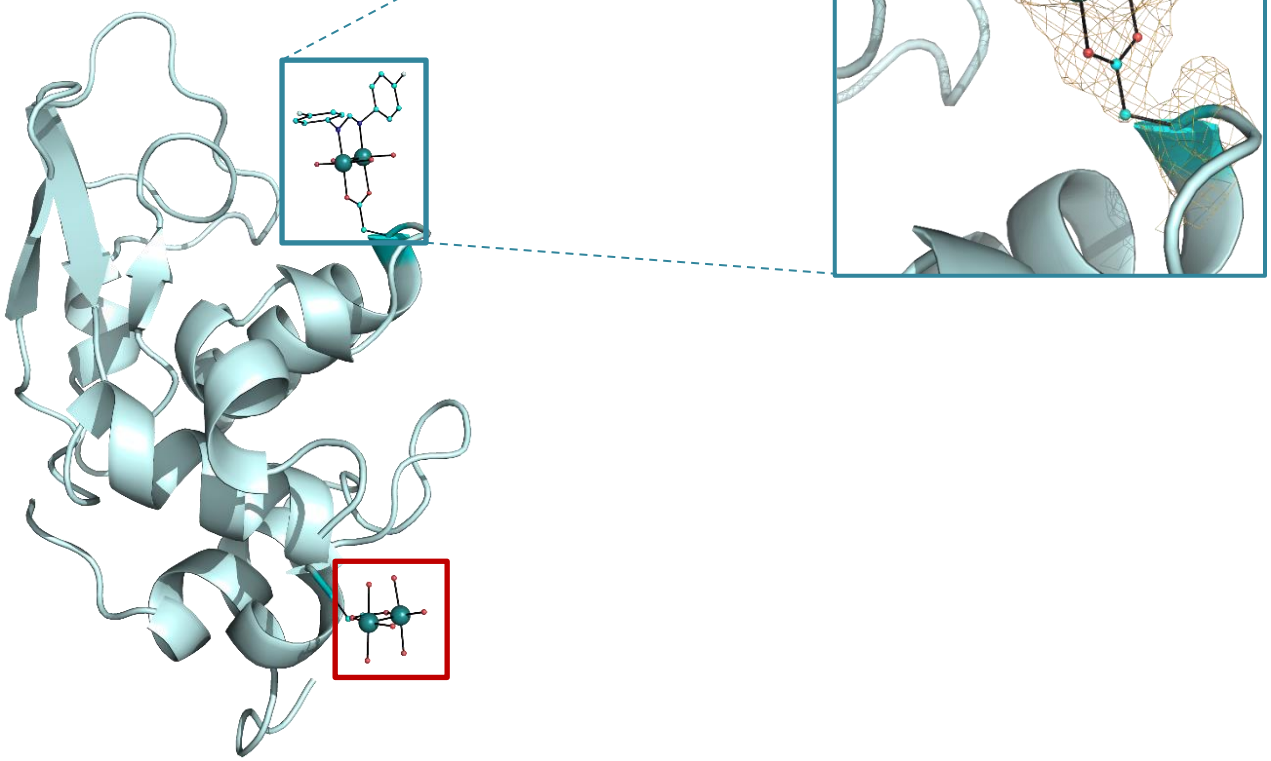

Site 1 → Asp101

Trans coordination to formamidinate ligand

Resolution	R-factor (R-free)	Condition
1.81 Å	0.223 (0.283)	2 M HCOONa, 0.1 M HEPES buffer (pH 7.5)

The $2F_o$-F_c electron density maps are contoured at 1σ level

Results and discussion

Structure A

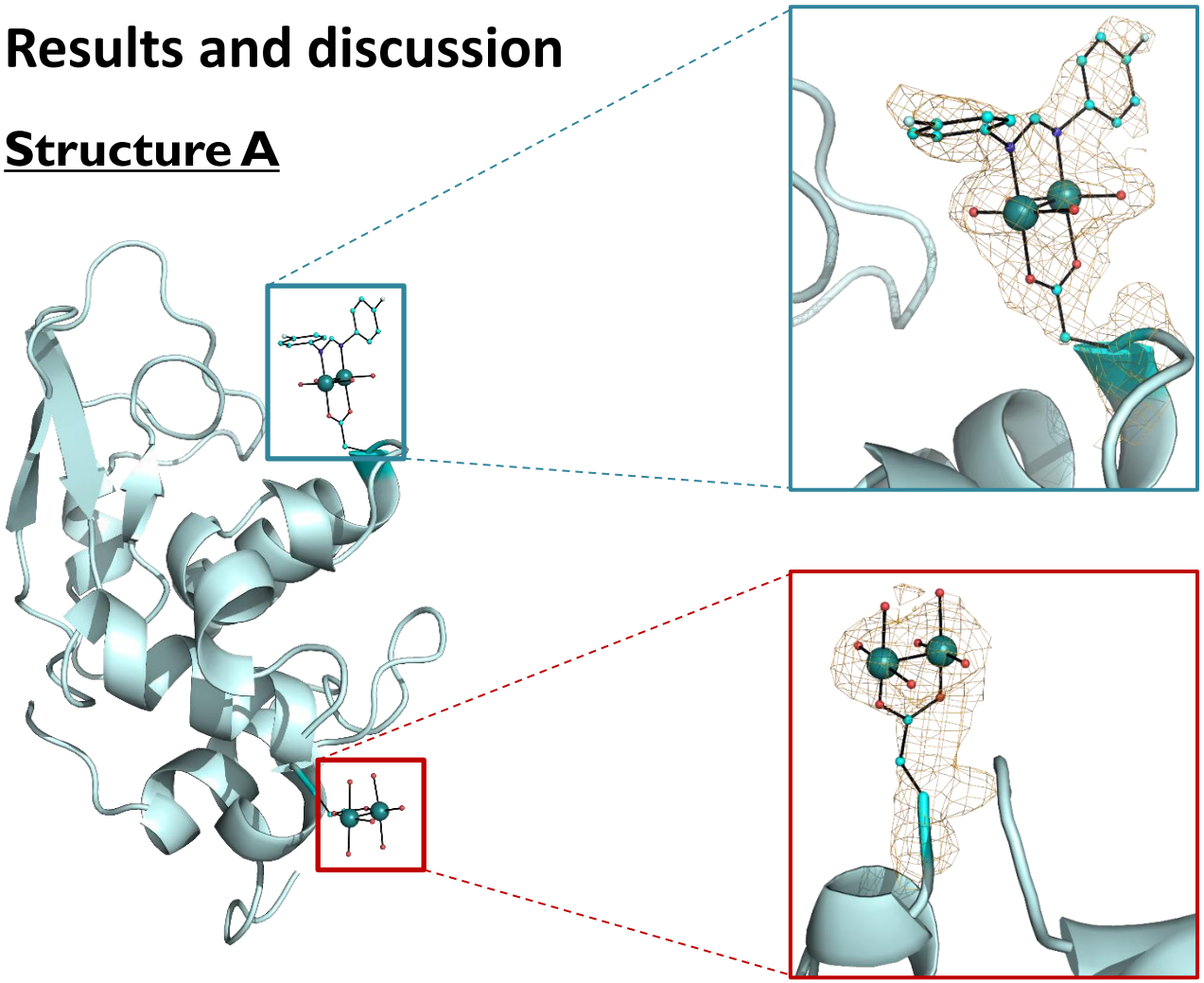

Site 1 → Asp101
Trans coordination to formamidinate ligand

Site 2 → Asp119

Resolution	R-factor (R-free)	Condition
1.81 Å	0.223 (0.283)	2 M HCOONa, 0.1 M HEPES buffer (pH 7.5)

The $2F_o$-F_c electron density maps are contoured at 1σ level

Results and discussion

Structure B

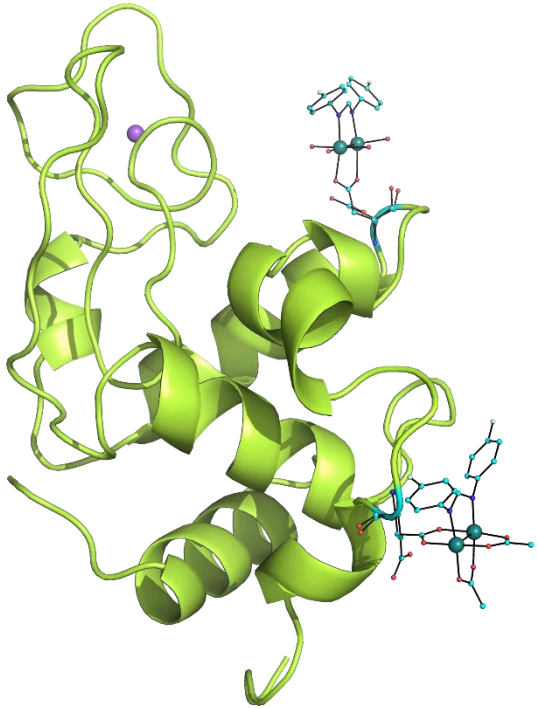

Resolution	R-factor (R-free)	Condition
1.38 Å	0.190 (0.233)	20 % Ethylene glycol CH_3COONa buffer (pH 4) $NaNO_3$ 0.6 M

Results and discussion

Structure B

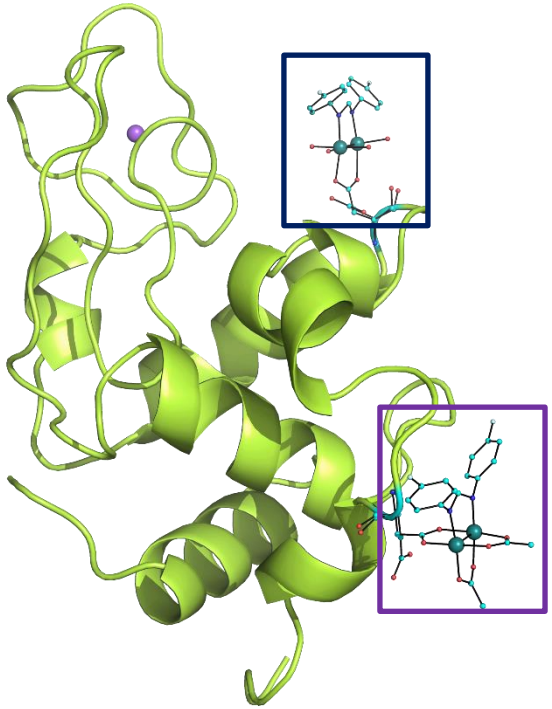

Resolution	R-factor (R-free)	Condition
1.38 Å	0.190 (0.233)	20 % Ethylene glycol CH_3COONa buffer (pH 4) $NaNO_3$ 0.6 M

Results and discussion

Structure B

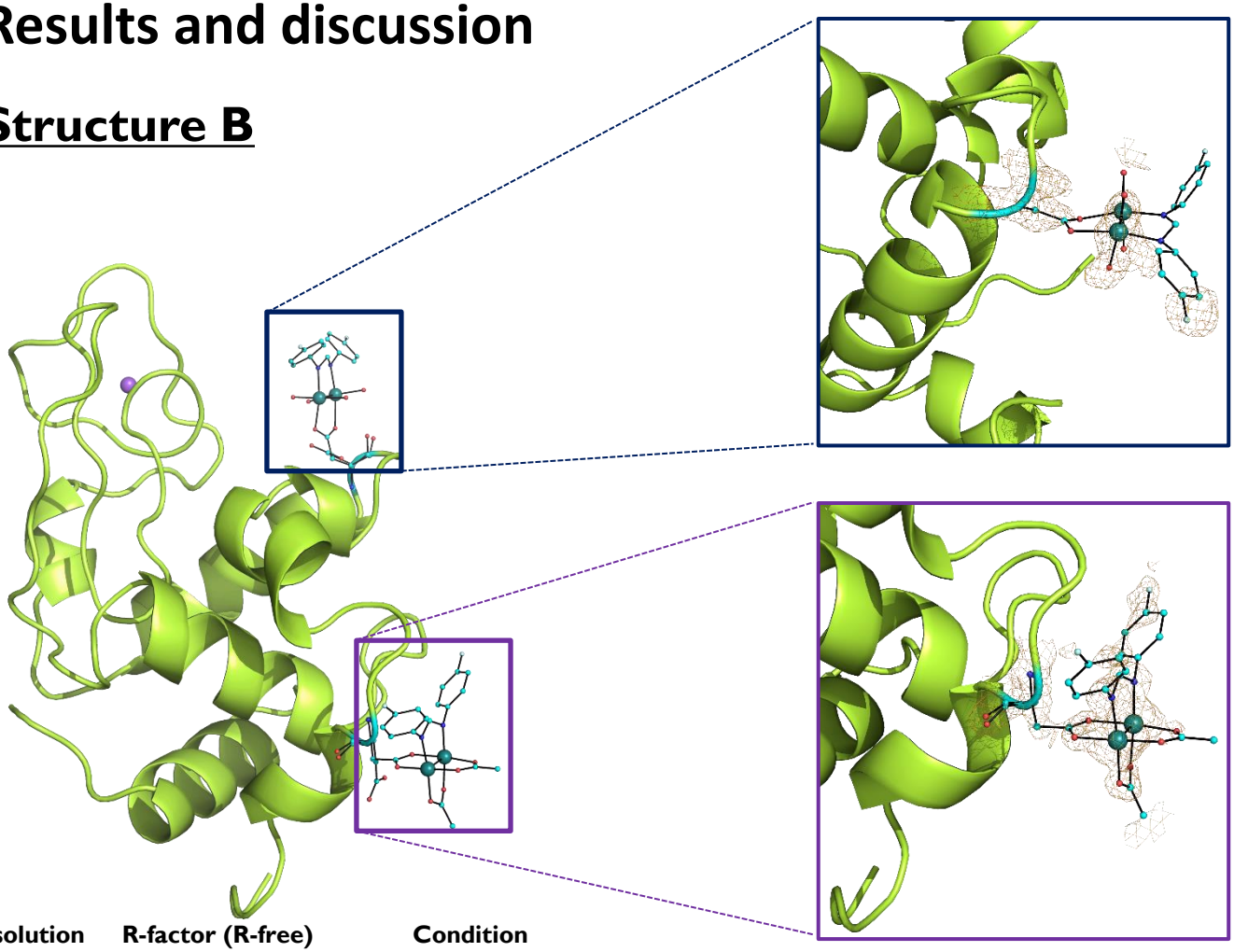

Site 1 → Asp101

Site 2 → Asp119

Resolution	R-factor (R-free)	Condition
1.38 Å	0.190 (0.233)	20 % Ethylene glycol CH_3COONa buffer (pH 4) $NaNO_3$ 0.6 M

The $2F_o$-F_c electron density maps are contoured at 1σ level

Results and discussion

Structure B

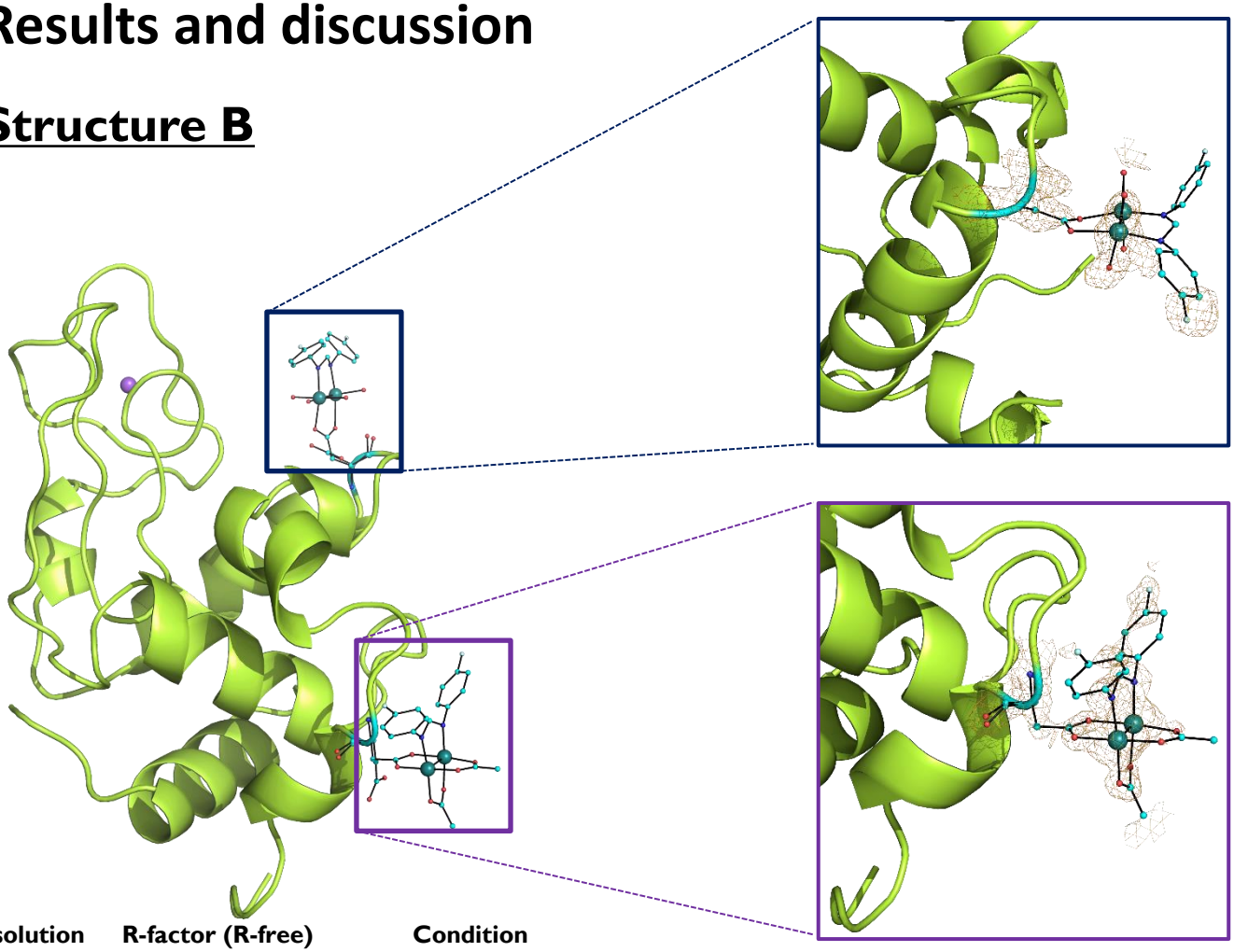

Site 1 → Asp101
Trans coordination to formamidinate ligand

Site 2 → Asp119
Cis coordination to formamidinate ligand

Resolution	R-factor (R-free)	Condition
1.38 Å	0.190 (0.233)	20 % Ethylene glycol CH_3COONa buffer (pH 4) $NaNO_3$ 0.6 M

The $2F_o$-F_c electron density maps are contoured at 1σ level

Results and discussion

Structure B

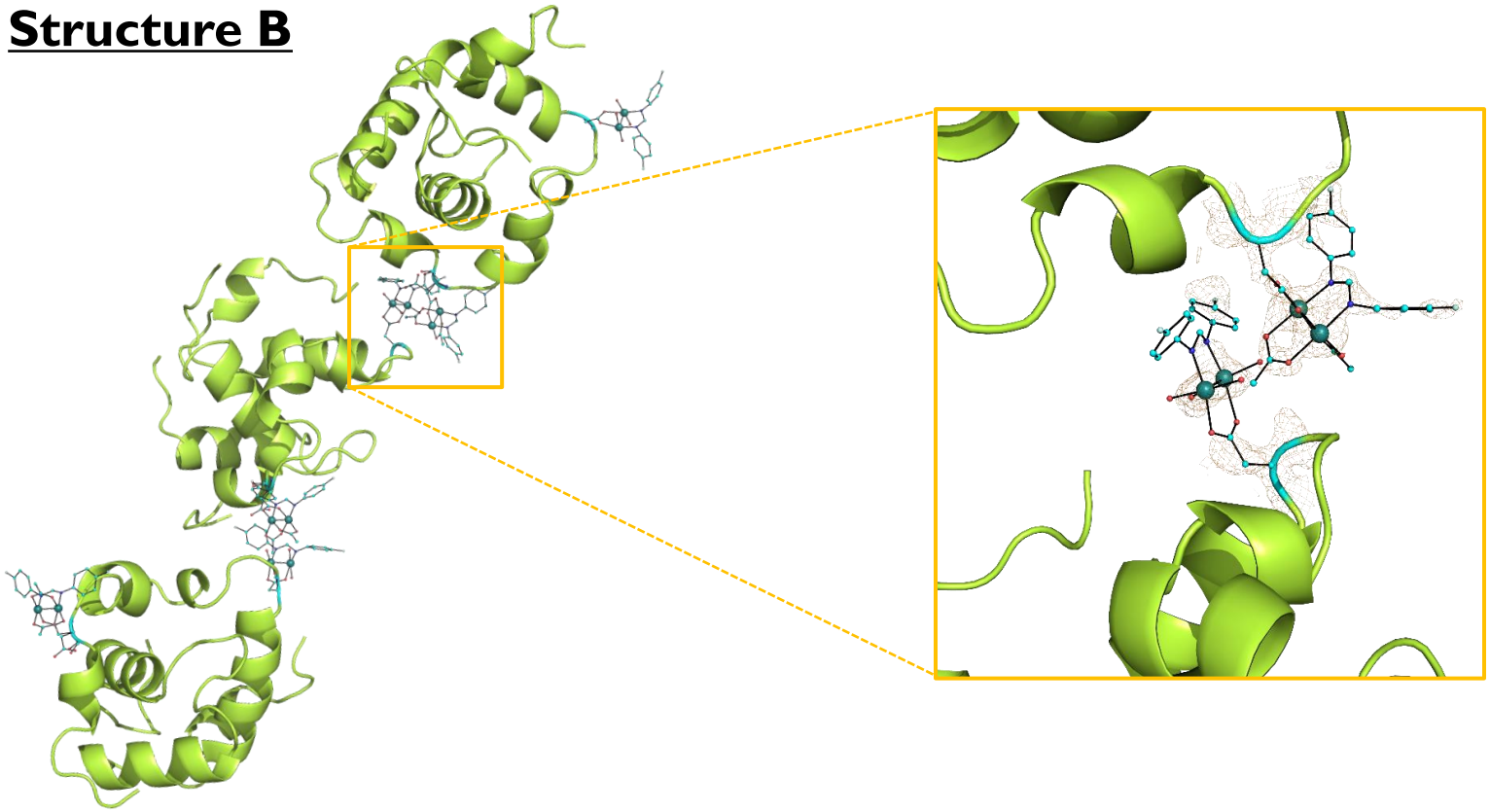

Resolution	R-factor (R-free)	Condition
1.38 Å	0.190 (0.233)	20 % Ethylene glycol CH_3COONa buffer (pH 4) $NaNO_3$ 0.6 M

The $2F_o$-F_c electron density maps are contoured at 1σ level

Results and discussion

Structure C

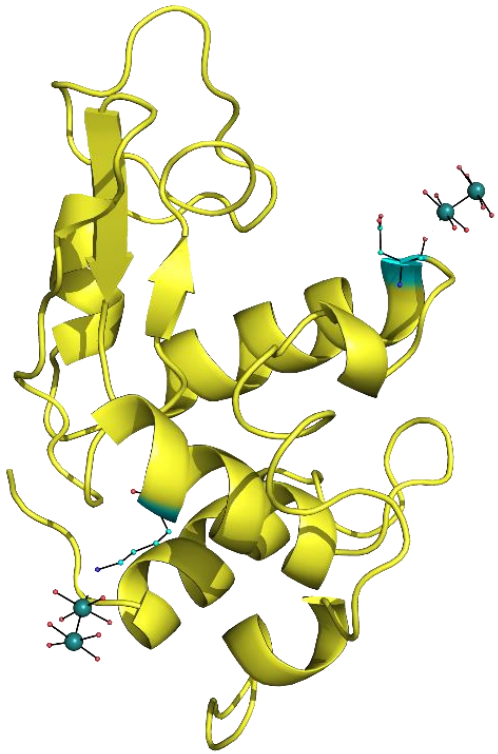

Resolution	R-factor (R-free)	Condition
1.07 Å	0.184 (0.214)	0.8 M Succinic acid (pH 7)

Results and discussion

Structure C

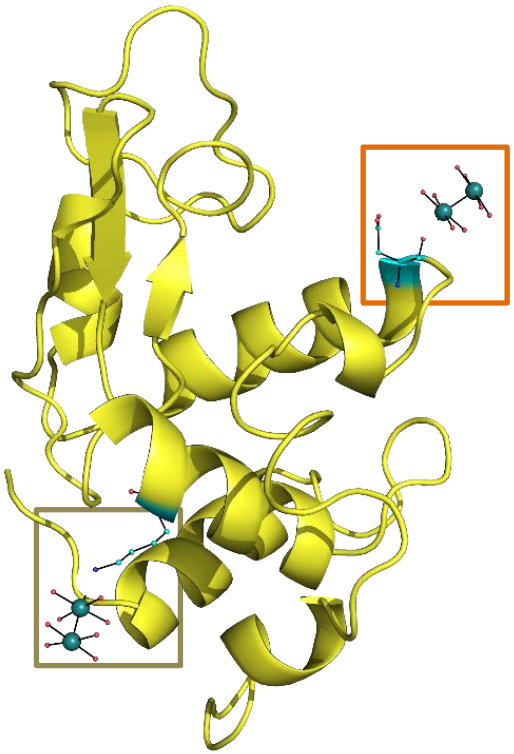

Resolution	R-factor (R-free)	Condition
1.07 Å	0.184 (0.214)	0.8 M Succinic acid (pH 7)

Results and discussion

Structure C

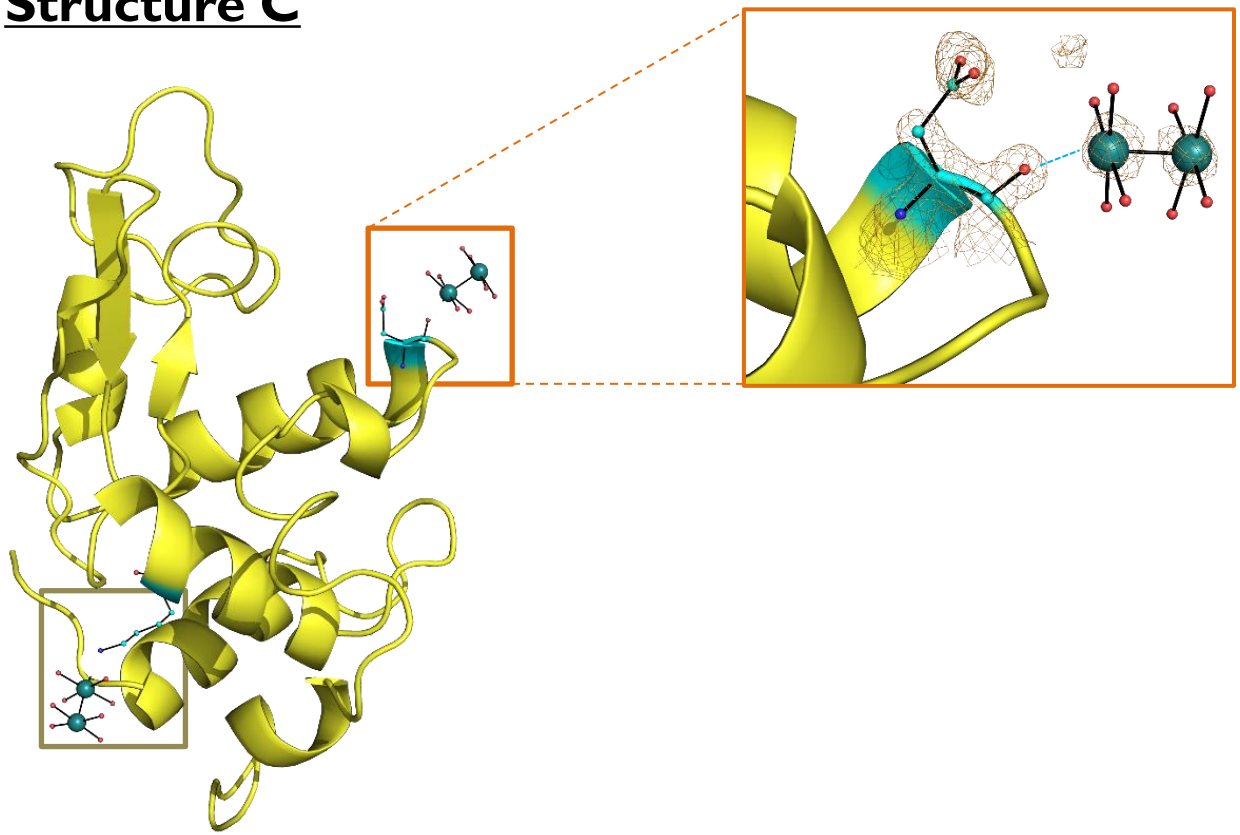

Site 1 → Asp 101
Axial interaction with the carbonyl group

Resolution	R-factor (R-free)	Condition
1.07 Å	0.184 (0.214)	0.8 M Succinic acid (pH 7)

The $2F_o$-F_c electron density maps are contoured at 1σ level

Results and discussion

Structure C

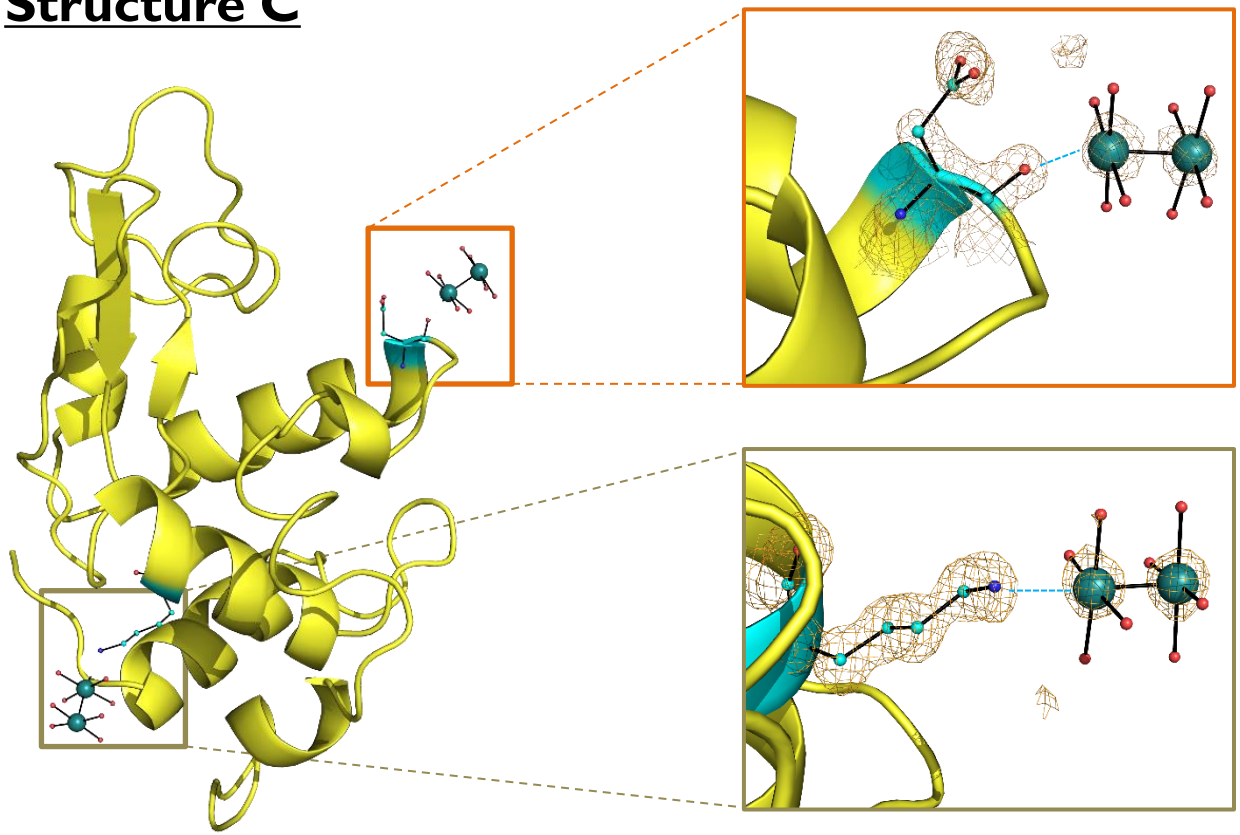

Site 1 → Asp 101
Axial interaction with the carbonyl group

Site 2 → Lys33
Axial interaction with the side chain of Lysine

Resolution	R-factor (R-free)	Condition
1.07 Å	0.184 (0.214)	0.8 M Succinic acid (pH 7)

The $2F_o$-F_c electron density maps are contoured at 1σ level

Conclusions

Novel structures of Ru_2-HEWL

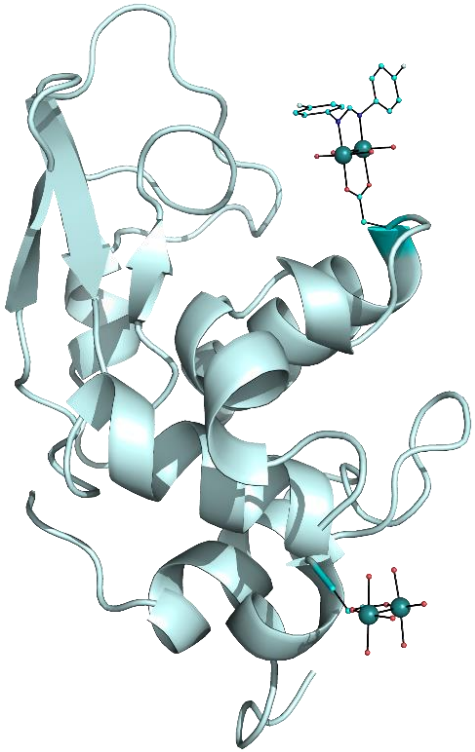

Structure A

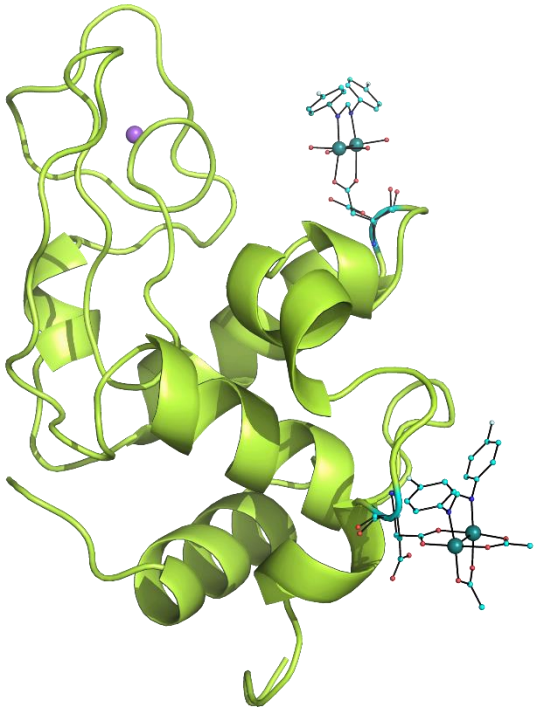

Structure B

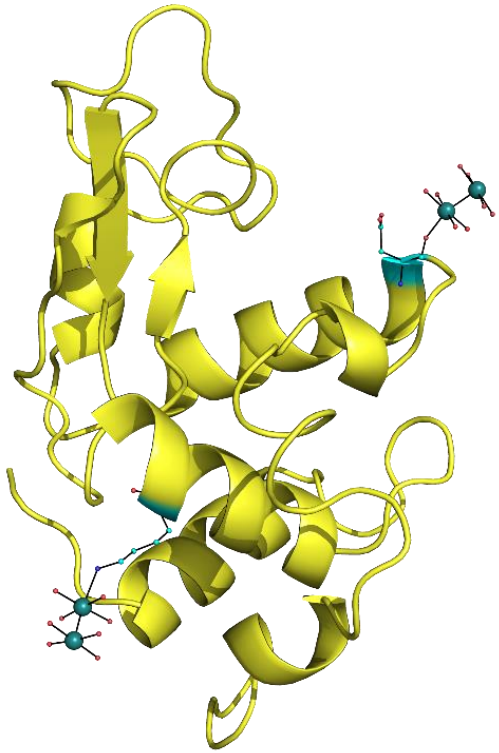

Structure C

Conclusions

Different coordination modes

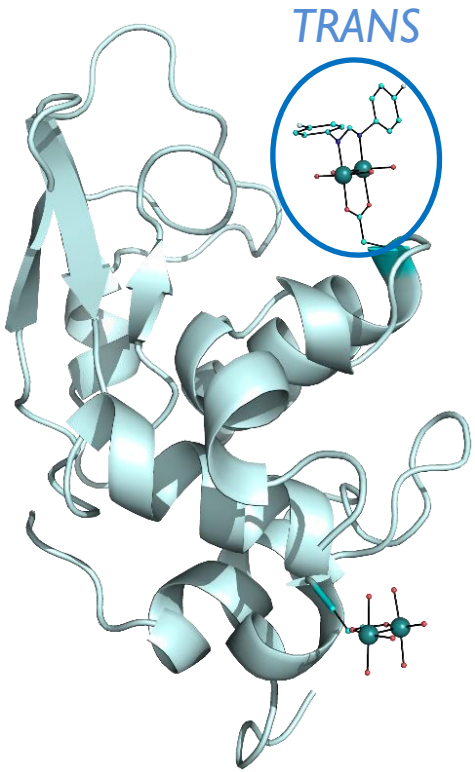

Structure A

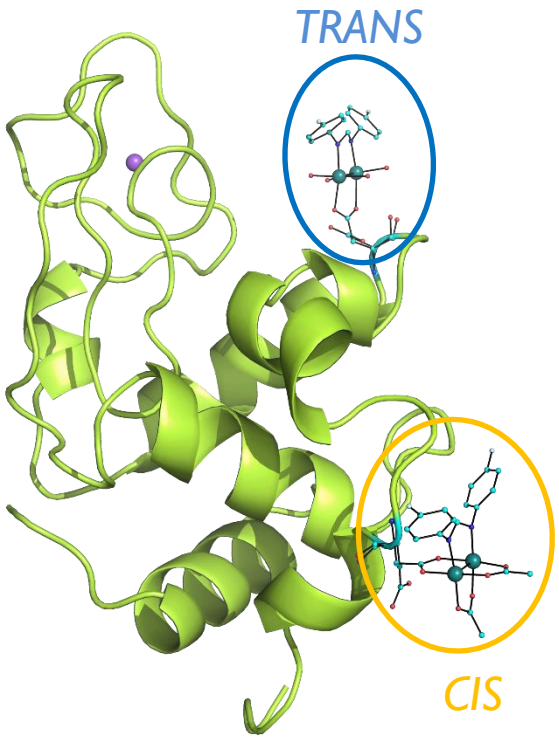

Structure B

Conclusions

Axial interaction Ru_2-HEWL

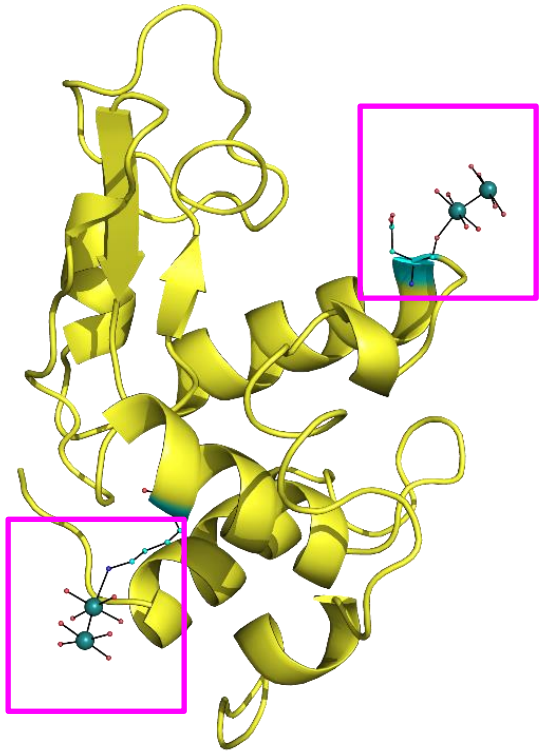

Structure C

Conclusions

Valuable information to design new metalloenzymes

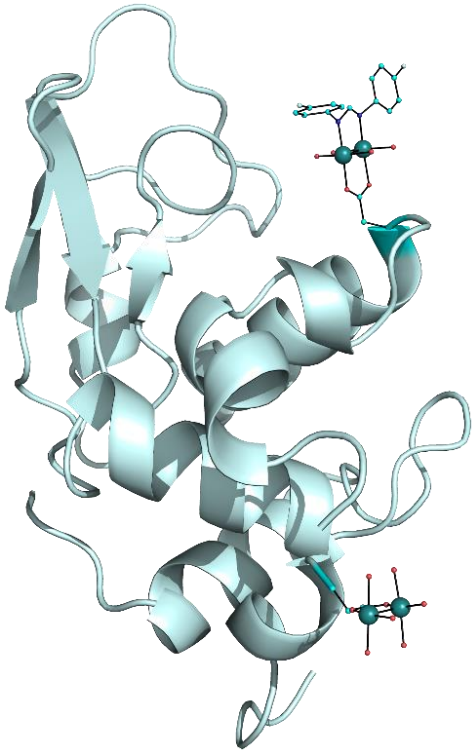

Structure A

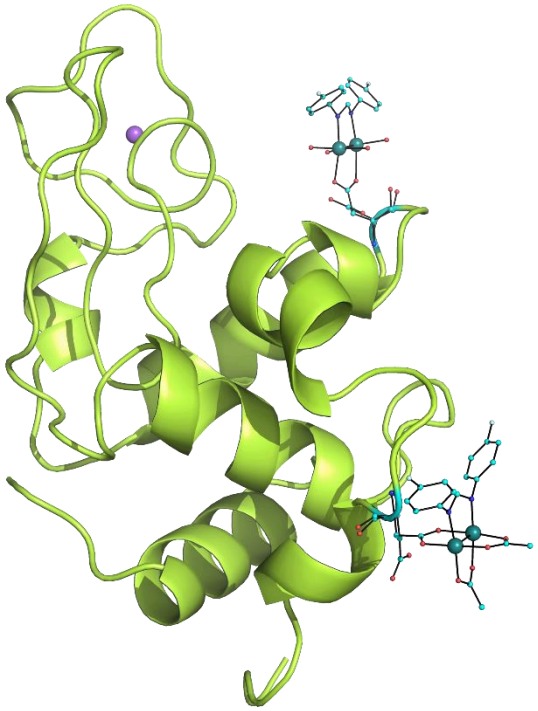

Structure B

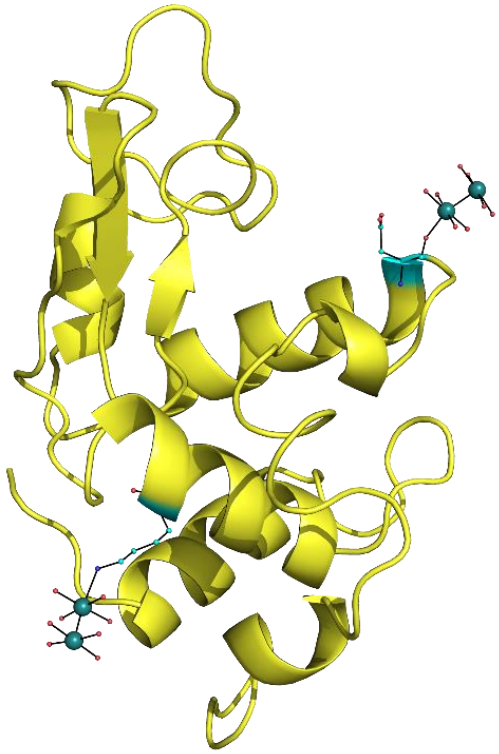

Structure C

Acknowledgments